

We are IntechOpen, the world's leading publisher of Open Access books Built by scientists, for scientists

6,100

Open access books available

149,000

International authors and editors

185M

Downloads

Our authors are among the

154

Countries delivered to

TOP 1%

most cited scientists

12.2%

Contributors from top 500 universities



WEB OF SCIENCE™

Selection of our books indexed in the Book Citation Index
in Web of Science™ Core Collection (BKCI)

Interested in publishing with us?
Contact book.department@intechopen.com

Numbers displayed above are based on latest data collected.
For more information visit www.intechopen.com



Chapter

Wind Tunnel Experiments on Turbulent Boundary Layer Flows

Adrián R. Wittwer, Acir M. Loredou-Souza, Jorge O. Marighetti and Mario E. De Bortoli

Abstract

The knowledge and experimental development of boundary layer turbulent flows is extremely important in applications related to the building aerodynamics, wind comfort, atmospheric dispersion, and even aeronautics. The Aerodynamic Laboratories of the UFRGS and UNNE have been making joint activities related to wind engineering such as those mentioned earlier for more than 25 years. In this work, a compilation of different experiments on turbulent boundary layer flows realized in these both laboratories is carried out. The characteristics of flows that develop on a smooth surface of the wind tunnel are experimentally evaluated. Then, reduced-scale models of atmospheric boundary layer flows are analyzed including the effects of turbulence generators and surface roughness. Special attention on the behavior of the turbulent parameters in the case of experimental studies using low mean velocity is paid. Finally, some comments referring to recent studies on thermal effects in turbulent boundary layer flows and the development of reduced-scale models of convective flows are included.

Keywords: wind engineering, aerodynamics, turbulence, scale models, smooth and roughness surface effects

1. Introduction

The wind tunnel is an experimental device for aerodynamic studies. Turbulent boundary layer flows are modeled within the test section of a wind tunnel in order to apply them to complex experimental studies. The physical simulation of atmospheric boundary layer (ABL) flows is one of the bases of wind engineering. That type of experimental procedure requires a careful investigation of the characteristic parameters of mean flow and turbulence. Different measurements must be carried out with specific equipment to be able to evaluate the velocity fluctuations of the turbulent flow.

Boundary layer flows are commonly characterized by their mean velocity and turbulent intensity profiles. The Prandtl logarithmic law (Eq. (1)), proposed from similarity theories, can be used to compare experimental results. In this mathematical expression, U is the mean velocity, u^* is the friction velocity, k is 0,4 (Kármán constant), and z_0 is known as the roughness height:

$$U(z)/u^* = (1/k)\ln(z/z_0) \quad (1)$$

Effects of the surface roughness, temperature, and others properties are transmitted by turbulent flows in case of the atmospheric boundary layer (ABL). Turbulent exchanges are very weak when there are very stable thermal stratification wind conditions [1]. The atmospheric boundary layer over nonhomogeneous terrain is not well defined because topographical features generate highly complex flows. The depth of the atmospheric boundary layer is only 100 m during stable nighttime conditions and could reach 1 km during unstable daytime conditions [2]. The aforementioned expression of Prandtl's law is modified when applied near the surface in the case of a neutral boundary layer (Eq. (2)). The zero-plane displacement z_d is then included for very rough surface:

$$U(z)/u^* = (1/k) \ln[(z - z_d)/z_0] \quad (2)$$

Another widely used expression used to characterize the vertical profile is the power law (Eq. (2)). The exponent α varies between 0.10 and 0.43, and the thickness of the boundary layer z_g ranges from 250 to 500 m, depending on the type of terrain [2]. This type of vertical velocity distribution is verifiable under conditions of neutral stability, which are those to be considered for the analysis of wind loads:

$$U(z)/U(h_g) = (z/h_g)^\alpha \quad (3)$$

The turbulence spectrum is the analytical tool used to investigate the velocity fluctuation characteristics of laboratory turbulent flows. Experimental spectra are fitting to some functional form to define dimensionless turbulence spectra in accordance with a similarity theory [3, 4]. Using similarity theory will allow the dimensionless spectra of atmospheric and laboratory flows to collapse, if the dimensionless spectra were formulated with the appropriate parameters [5].

2. Boundary layer wind tunnels

The most efficient tool to experimental study of aerodynamic phenomena is the wind tunnel. Basically, there are three types of wind tunnels. Aerodynamic tunnels, called the "first generation" of wind tunnels, are mainly used in aeronautics and vehicular applications. Boundary layer tunnels, called "second generation," are used for studies involving atmospheric boundary layer (ABL) flows. Finally, the "third generation" of wind tunnels is beginning, the three-dimensional tunnels, in which different types of flow can be simulated. An example of the "third generation" of wind tunnels is the WindEEE Dome [6, 7], a hexagonal wind tunnel with 25 m in diameter and 40 m in diameter for the external return built in recent years in Canada.

In this work, measurements of flow velocity realized in two different boundary layer wind tunnels will be used for the experimental analysis. The closed-return wind tunnel "Prof. Joaquim Blessmann" of the Laboratório de Aerodinâmica das Construções, Universidade Federal de Rio Grande do Sul, UFRGS, Brazil [8] and the "Jacek Gorecki" open-circuit wind tunnel of the Laboratorio de Aerodinámica, Universidad Nacional del Nordeste, UNNE [9] are the boundary layer tunnels employed to develop the experiments. Both wind tunnels can be considered as low-speed tunnels.

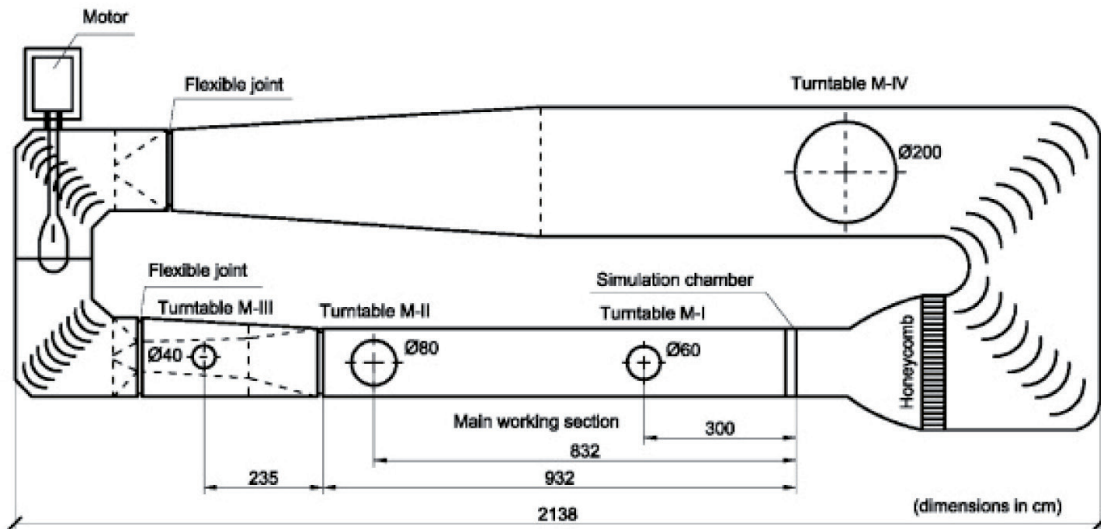


Figure 1.
 The “Prof. Joaquim Blessmann” boundary-layer wind tunnel of the UFRGS.

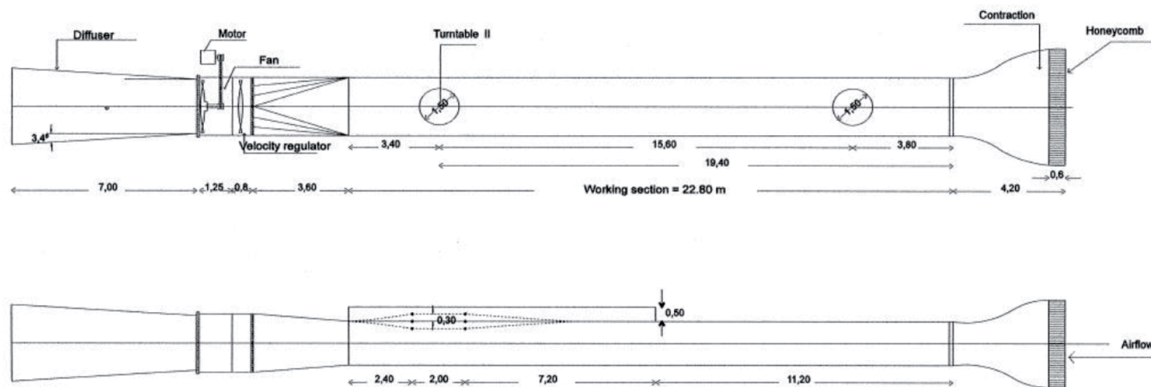


Figure 2.
 The “Jacek Gorecki” boundary-layer wind tunnel of the UNNE.

The “Prof. Joaquim Blessmann” wind tunnel of UFRGS has a cross section of 1.30 m 0.90 m at downstream end of the main working section that has 9.32 m long (**Figure 1**). Characteristics and performance of this wind tunnel are described by Blessmann [9]. The “Jacek Gorecki” UNNE wind tunnel is a 39.56 m-long channel, and the test section is a 22.8-m-long rectangular chamber (2.40 m width × 1.80 m height) with two rotating tables to place test models (**Figure 2**).

3. Boundary layer flows on smooth surface

In this first part, we show the behavior of the boundary layer that develops on the smooth surface (floor) of a wind tunnel. Different measurements were made in both wind tunnels, the J. Blessmann tunnel at UFRGS and the J. Gorecki tunnel at UNNE, where different wind speeds were used. **Figure 3** shows the general characteristics of the interior of both tunnels, with the dimensions of the test chamber being 1.30 m width × 0.90 m high × 9.32 m long for the UFRGS tunnel and 2.40 m width × 1.80 m high × 22.8 m long for the UNNE tunnel, respectively.

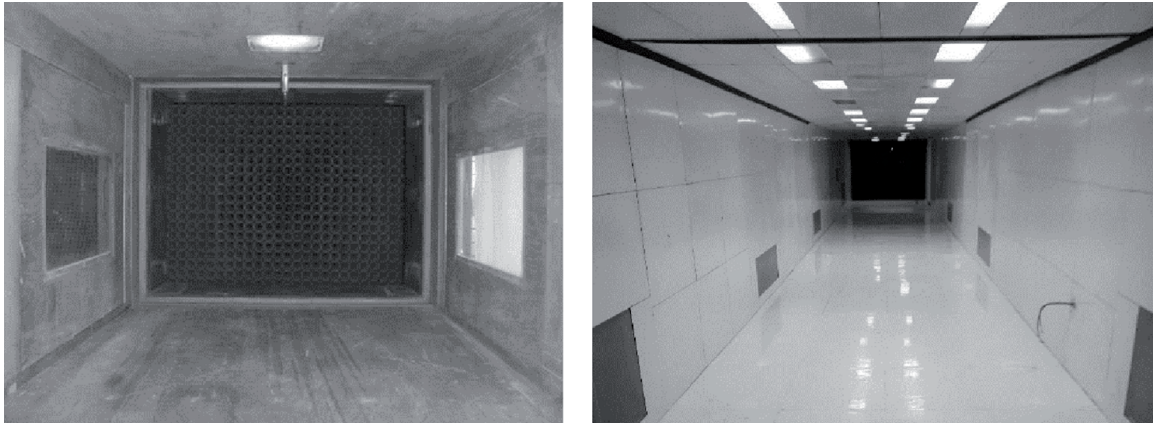


Figure 3. Test sections for smooth surface experiments at the UFRGS wind tunnel (left) and at the UNNE wind tunnel (right).

Experiments.	Position	U_{ref} [m/s]	H_{BL} [m]	Re_H
UFRGS -TI	Center line	38.9	0.075	1.95×10^5
UNNE -TI	Center line	22.7	0.130	1.97×10^5
UFRGS -TII	Center line	39.5	0.125	3.29×10^5
UNNE -TII - 00	Center line	24.5	0.300	4.90×10^5
UNNE -TII - 06(L)	Left side	24.5	0.300	4.90×10^5
UNNE -TII - 06(R)	Right side	24.5	0.300	4.90×10^5
UFRGS-LV1	Center line	0.9	0.175	1.05×10^4
UFRGS-LV2	Center line	2.1	0.150	2.10×10^4
UFRGS-LV5	Center line	4.7	0.150	4.70×10^4

Table 1. Characteristic parameters of the smooth surface experiments.

The different experiments used to characterize the smooth surface boundary layer flow are described in **Table 1**. TI and TII refer to rotating Tables I and II of each tunnel (positions of rotating tables are indicated in **Figures 1** and **2**). Most of the measurements were made in the central position of the test chamber, but for the UNNE tunnel, two measurements are indicated at 0.6 m to the left (L) and right (R) of the central position in order to illustrate the lateral homogeneity. Each experiment is considered stationary, and it is characterized by the reference velocity U_{ref} measured at the top of the boundary layer, the boundary layer height H_{BL} , and the Reynolds number Re_H .

All measurements were made with a constant temperature hot-wire anemometer. Acquisition time and sampling frequency of the velocity records were modified in each case according to the type of boundary layer flow and the reference speed of the experiment. These values are indicated later in the text where the description and analysis of the different experiments are made. In the case of the experiments carried out at UFRGS, the CTA System Data Acquisition System—DANTEC-Stream-Line Pro [10] was used. On the other hand, the measurements at UNNE were made by a Dantec 56C constant temperature hot-wire anemometer connected to a Stanford

amplifier with low- and high-pass analogic filters. Hot-wire signals were digitalized by a DAS-1600 A/D converter board controlled by a computer which was also used for the analysis of the results. Voltage output from hot wires was converted in mean velocity and velocity fluctuations [11, 12] by the probe calibration curves previously determined.

3.1 High-velocity measurements

Firstly, the mean speed and turbulence intensity profiles obtained with relatively high speeds, between 20 and 30 m/s, shown in **Figure 4** are analyzed. Velocity profiles are dimensionless with the reference velocity measured “outside” the boundary layer, where the mean velocity remains approximately constant. The vertical coordinate z is not dimensionless in order to show how the height of the boundary layer varies in each case. In this way, we can observe that the UNNE tunnel, where the cross section of the test section has larger dimensions, the thicknesses of the boundary layer generated are relatively greater. Likewise, it is observed that in the rotating Table I, located at the beginning of the test section, the boundary layer thicknesses developed in both tunnels are less than the thicknesses obtained in the rotating Table II.

The fluctuating speed records measured with a hot-wire anemometer have a duration of 60 seconds in the tests carried out in the UFRGS tunnel and 90 seconds in the tests carried out in the UNNE tunnel. The acquisition frequency of the velocity records is 2048 Hz for the UFRGS measurements and 3000 Hz for the UNNE measurements. Finally, low-pass filtering was implemented for the analog signals measured at UNNE, while low-pass filtering was not used for the UFRGS measurements.

Velocity profiles indicate a fairly harmonic velocity distribution and even good lateral homogeneity, with respect to flow quality. The maximum turbulence intensities

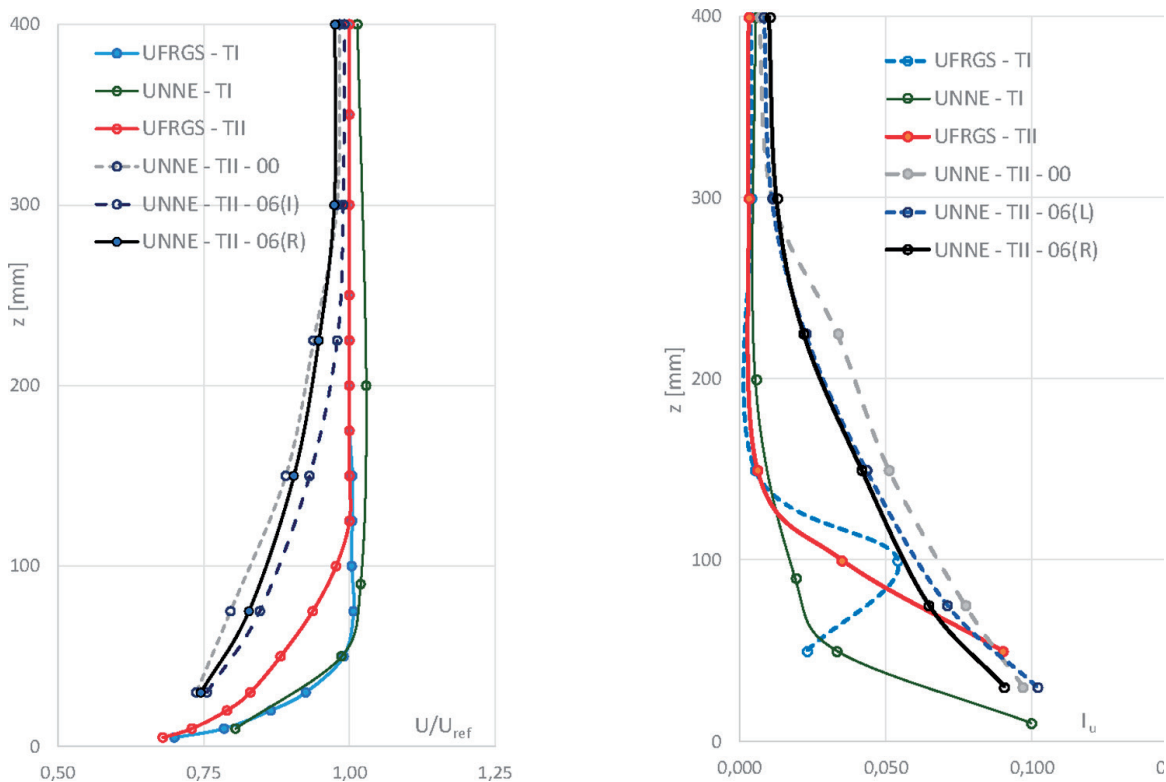


Figure 4. Mean velocity and turbulence intensity profiles for smooth surface experiments (high velocity).

measured at distances of 15 to 30 mm from the floor do not exceed values of 10% and “outside” the boundary layer are less than 1%. In general, the vertical distribution shows a fairly harmonic behavior, except in the measurements corresponding to rotating Table I—UFRGS wind tunnel, where a localized increase is observed for height $z = 100$ mm, possibly due to a vortex shedding phenomena located at the convergent.

3.2 Low-velocity measurements

The mean velocity and turbulence intensity profiles for relatively lower mean velocities are now analyzed. All fluctuating speed records used for the low-speed analysis have a duration of 180 seconds, and the acquisition frequency for the speed records is 2048 Hz. These records come from the tests carried out on the rotating Table II of the UFRGS tunnel, and the corresponding analog signals do not include low-pass filtering.

The analysis of the vertical distribution of the mean velocity (**Figure 5**) shows an increase in the thickness of the boundary layer when the velocity decreases from 150 mm ($U_{ref} = 4.7$ m/s - LV5) to approximately 200 mm ($U_{ref} = 0.9$ m/s - LV1). The profile obtained with the lowest speed (LV1) presents a more irregular behavior than the others, probably because the effects of viscosity are more noticeable. **Figure 5** also includes the profile obtained on Table II of the UFRGS tunnel at high speed ($U_{ref} = 39.5$ m/s - TII - HV) to compare and verify a more harmonic behavior when the mean flow speed is higher.

The turbulence intensity profiles accompany the behavior shown by the average speeds. The highest values of I_u obtained up to 200 mm height correspond to the measurements of lower speed (LV1). However, the measurement point closest to the tunnel floor shows a slight decrease in I_u with respect to the one immediately above it (from 0.13 to 0.10) as a result of viscous effects.

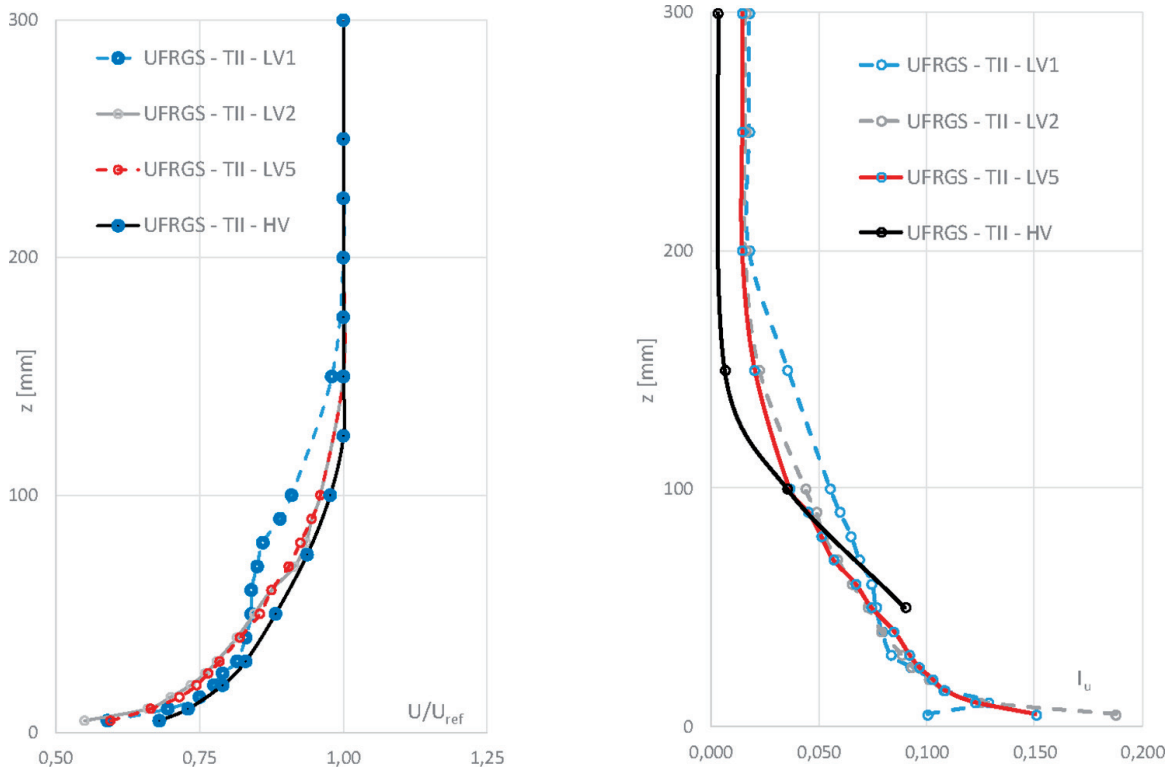


Figure 5. Mean velocity and turbulence intensity profiles for smooth surface experiments (low velocity).

3.3 Spectral analysis

Spectral results from longitudinal velocity fluctuations were obtained by Fourier analysis applied to different sampling series, obtained in the UNNE wind tunnel (high velocity) and UFRGS wind tunnel (low velocity). Time acquisition and sampling frequency are given in **Table 2**. The obtained series were divided in blocks to which a fast Fourier transform (FFT) algorithm was applied [13]. Three spectra obtained at the UFRGS wind tunnel and a spectrum measured at the UNNE wind tunnel are shown in **Figure 6**. Values of the spectral function decrease as the mean velocity also decreases. The spectrum obtained at the measurement point closest to the tunnel floor with low speed allows verification of the behavior observed in the turbulence intensity profile (it shows a slight decrease in I_u at this point with respect to the immediately higher one). Viscous attenuation effects start around 10 Hz at this measurement point. An important characteristic of the spectra measured with high velocity is the presence of a clear region with a $-5/3$ slope, characterizing Kolmogorov's inertial subrange.

4. Physical models of the atmospheric boundary layer

Jensen [14] established in 1958 that: "The correct model test with phenomena in the wind must be carried out in a turbulent boundary layer, and the model-law requires that this boundary layer be to scale as regards the velocity profile." Later studies on physical reduced-scale models of atmospheric boundary layer attempted to reproduce as closely as possible the mean flow and turbulence structure of the atmospheric flow, in particular, those properties related to neutral atmospheric boundary layer and wind loading effects.

In the preceding section, it was verified that the boundary layer thickness achieved with a smooth surface is relatively small. Structural model tests require higher boundary layer thicknesses and turbulence structures representative of atmospheric winds. This problem gave rise to different methods of physical simulation of atmospheric flows in a wind tunnel.

The general similarity requirements for reproducing ABL flows in wind tunnels are geometric, kinematic, dynamic, thermal, and boundary conditions similarity. In terms of dimensionless parameters, it is necessary to maintain the equality of Reynolds, Richardson, Rossby, and Prandtl numbers, in addition to geometric similarity and boundary conditions [15].

The fluid used in wind tunnels for ABL simulation is air, so the Prandtl number is automatically the same in the model and prototype. On the other hand, Rossby number equality cannot be considered in conventional tunnels, so applications are restricted to flow conditions where the effects of terrestrial rotation are negligible.

Experiments	Time [s]	Sampling frequency [Hz]	Low-pass filter [Hz]
UFRGS -TII - LV1	180	2048	—
UFRGS -TII - LV5	180	2048	—
UNNE - TII - HV	60	3000	1000

Table 2.
 Characteristic parameters of time series for spectral analysis.

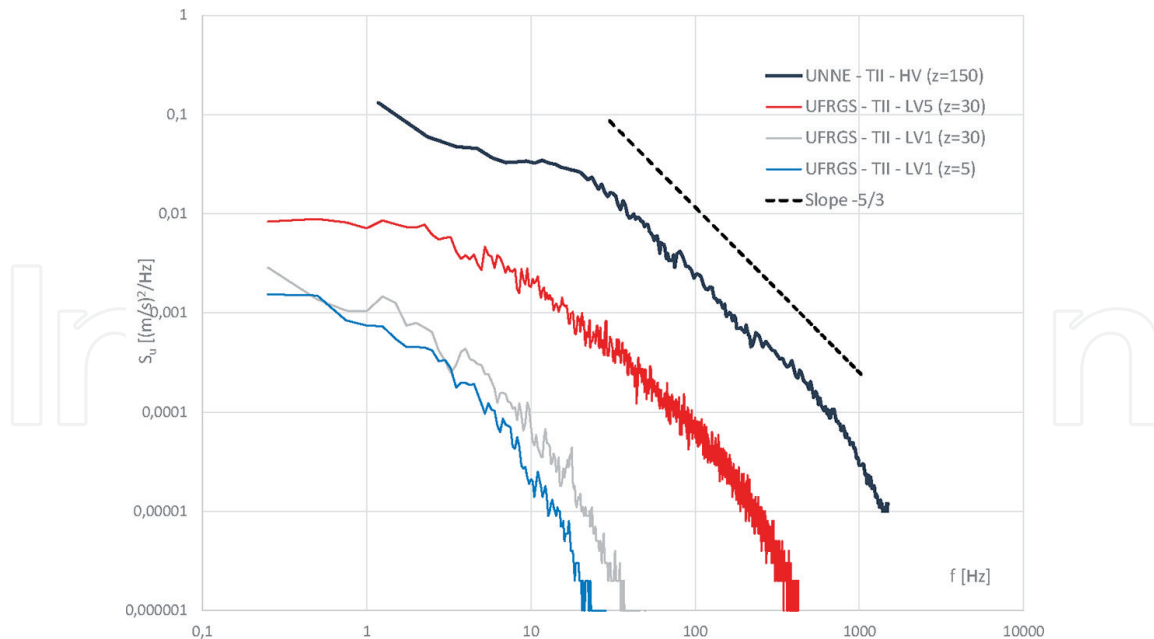


Figure 6.
Spectra for smooth surface experiments (low and high velocity).

The Reynolds number is usually much smaller in the wind tunnel than the real scale, so the equality condition is relaxed. The aim is simply to reach values high enough to obtain the aerodynamic similarity of the phenomenon. Finally, the Richardson number describes the relationship between thermal and mechanical turbulence [16], establishing the difference between thermally stratified and neutral boundary layers.

4.1 Wind tunnel simulation of atmospheric neutral boundary layer

Counihan [17] and Standen [18] have developed simulation techniques particularly suitable for reproducing ABLs in neutral stability employing the roughness, barrier, and blending methods. These techniques make it possible to obtain representations of the boundary layer flows that are generated over rural and urban terrains. Particularly, Standen technique allows the full-depth and part-depth simulations of ABL. Thus, it is possible to change the model scales for the tests.

These physical models of ABL under neutral stability conditions behave well at the relatively high speeds used in wind tunnels for aerodynamic loading studies. Atmospheric dispersion tests must be carried out at lower speeds, and it is normal for exaggerated speed fluctuations to occur in the low-frequency region of the turbulence spectrum. These fluctuations do not reproduce the characteristics of atmospheric wind [19]. For this reason, it is necessary to make a more thorough evaluation of the wind tunnel performance before carrying out diffusion studies [20]. Most studies in wind tunnels are carried out using simulations of neutral ABL; however, atmospheric thermal stratification must be considered in some cases. The drawback of modeling thermal stratification is the requirement of a large investment in equipment for its development. A relatively simple way of considering some non-neutral flow characteristics was proposed by Janssen [21] by modifying the layout and roughness elements of a simulation of neutral characteristics.

Next, some experimental results obtained in ABL simulations carried out in the UFRGS and UNNE wind tunnels are shown and analyzed.

4.2 Experimental analysis on atmospheric boundary layer models

A first ABL simulation method (UFRGS – S1) was applied at the UFRGS wind tunnel. Four perforated spires, a barrier and surface roughness elements were used to simulate a full-depth boundary layer. The arrangement of the simulation hardware is shown in **Figure 7** (left).

Then, an ABL full-depth simulation (UNNE – S2) was implemented in the UNNE tunnel based on the Counihan method. Four high elliptic vortex generators and a barrier were used, together with prismatic roughness elements placed on the test section floor along 17 m (see **Figure 7**—center). Finally, two Irwin-type generators separated 1.5 m were used to simulate the part-depth boundary layer by means of the Standen method (UNNE – S3). The windward plate of the simulator has a trapezoidal shape. The roughness elements distributed on the test section floor are the same that were used for the Counihan method (**Figure 7**—right).

Five experiments were analyzed to characterize the modeled boundary layer flow in each simulation. Different average speeds were evaluated only for simulation UFRGS – S1. Characteristic parameters of the different experiments on ABL simulations are indicated in **Table 3**.

Figure 8 shows the mean speed and turbulence intensity profiles for the five cases analyzed. The vertical z positions are dimensionless (the reference height H_{ref} is the boundary layer thickness). The vertical non-dimensionalization allows a better comparison of the profiles obtained in both wind tunnels and also of the different simulation methods used. The velocity profiles show a fairly harmonic behavior and the values remain consistent with those obtained by the power law using exponents 0.23 and 0.25. The I_u profiles indicate a distortion of the values in the two low-speed cases,

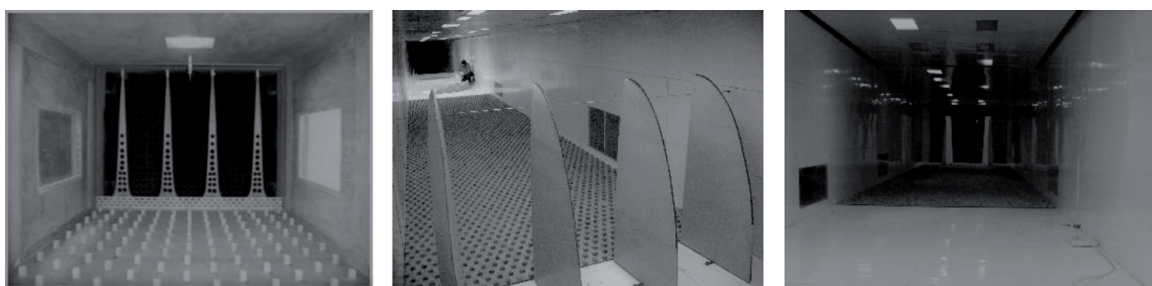


Figure 7. Simulation hardware: Perforated spires, barrier, and roughness (UFRGS – S1); Counihan method (UNNE – S2); Standen method (UNNE – S3).

Experiment	Position	U_{ref} [m/s]	H_{ref} [m]	Re_H
UFRGS – S1 – HV	Center line	35	0.60	1.40×10^6
UFRGS – S1 – LV1	Center line	1	0.60	4.00×10^4
UFRGS – S1 – LV2	Center line	3.5	0.60	1.40×10^5
UNNE – S2 – HV	Center line	27.5	1.17	2.15×10^6
UNNE – S3 – HV	Center line	25.3	1.21	2.04×10^6

Table 3. Characteristic parameters of the experiments on ABL models.

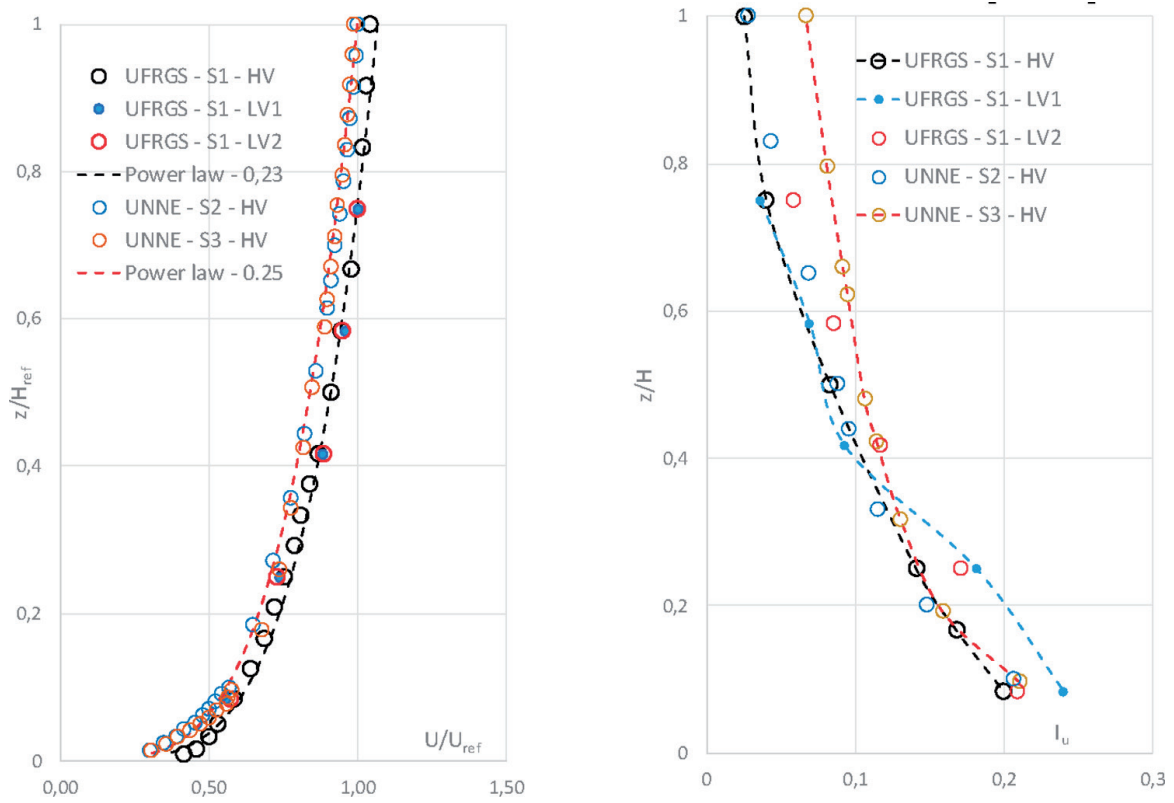


Figure 8. Mean velocity and turbulence intensity profiles for atmospheric boundary layer models.

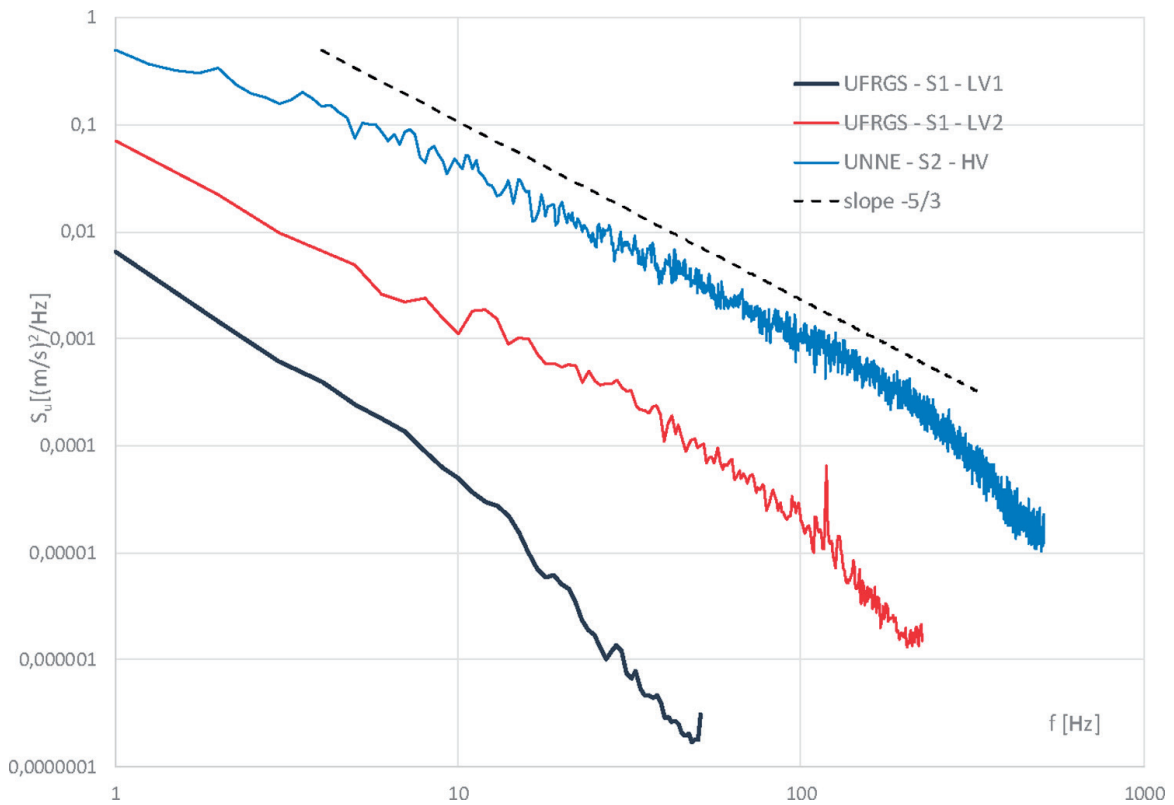


Figure 9. Spectra for atmospheric boundary layer models (low and high velocity).

mainly in the lowest speed one (UFRGS – S1 – LV1). On the other hand, an increase in turbulence levels is observed from $z/H \approx 0.3$ for the profile corresponding to part-depth simulation. This is consistent with the proposed model (part-depth) that aims to simulate the lower part of the ABL where the turbulence intensities are higher.

Two spectra obtained at low speed at the position $z/H = 0.25$ are shown in **Figure 9** to verify the energy distribution when the mean velocity decreases. Fluctuating velocity records used for the spectral analysis were acquired with a sampling frequency of 1024 Hz. These two spectra are compared with the spectrum obtained at high speed at the position $z/H = 0.15$. A poor definition of the Kolmogorov's inertial subrange is observed for the spectra measured at velocity $U_{\text{ref}} = 1$ m/s.

The objective of the evaluation of the mean flow, the turbulent parameters, and the spectral analysis is the general comparison between simulations carried out in two different tunnels, implemented with different methods and analyzed for different mean speeds. A comparison with data measured in the atmosphere is not intended. This type of analysis requires the non-dimensionalization of the spectra for their comparison with atmospheric spectra (see [22, 23]).

4.3 Some comments about stratified boundary layer

Most of the wind tunnel simulations do not include some effects measured in field experiments, such as vertical thermal flows due to the presence of solar radiation and other thermal sources [24–26]. The physically relevant quantities in turbulent winds are horizontal and vertical wind speeds, vertical temperature, pressure profile, and humidity distribution. These quantities are subject to fluctuations due to the flow dynamics and due to the complex conditions of the boundary layer [27]. The experiments in the wind tunnel use mechanical and thermal forces to simulate realistic ABL as observed in the literature [28, 29].

A recent study carried out in the UFRGS wind tunnel includes thermal effects in experiments that simulate a boundary layer. To carry out this work, a sector of the wind tunnel test section was equipped with a metal sheet and Peltier elements attached to it. Peltier elements heat or cool the floor of the wind tunnel depending on the polarity. Thus, heating the floor simulates the effects of solar radiation. Thermal effects generating new flow patterns become feasible to realize comparisons of wind tunnel simulations to stratified boundary layer conditions [30].

This work realized in the UFRGS Aerodynamics Laboratory presents and discusses the turbulent energy spectrum of the velocity fluctuations obtained with different mean incident wind velocities [31]. Smooth wind tunnel floor measurements were repeated under the same conditions with floor roughness. The time series of the longitudinal velocity component is determined with hot-wire anemometry and analyzed using the Hilbert-Huang transform method. Both neutral and convective wind tunnel boundary layers are considered in this study.

5. Final considerations

This work presents a compilation of different experiments on turbulent boundary layer flows realized in the UFRGS and UNNE wind tunnels. First, boundary layer flows developed on a smooth surface of the wind tunnel test section are

experimentally evaluated; next, some scale models of neutral ABL developed by different methods are analyzed. General characteristics and turbulence spectra are determined considering the effects of the average velocity variation and the influence of the dimensions of the test section. Finally, some studies on thermal effects in turbulent boundary layer flows developed in wind tunnels are analyzed. Specifically, a work recently carried out in the UFRGS tunnel to evaluate the thermal and roughness effects is analyzed and commented.

Acknowledgements

The authors acknowledge the technical personnel of the Laboratório de Aerodinâmica das Construções, Universidade Federal de Rio Grande do Sul (UFRGS, Brazil) and of the Laboratorio de Aerodinámica, Universidad Nacional del Nordeste (UNNE, Argentina).

This research was partially funded by Conselho Nacional de Desenvolvimento Científico e Tecnológico (CNPq, Brazil), Secretaría General de Ciencia y Técnica of the Universidad Nacional del Nordeste (SGCYT-UNNE, Argentina) and Facultad de Ingeniería of the Universidad Nacional del Nordeste (FI-UNNE, Argentina).

Author details


Adrián R. Wittwer^{1*}, Acir M. Loredou-Souza², Jorge O. Marighetti¹
and Mario E. De Bortoli¹

1 Facultad de Ingeniería, Universidad Nacional del Nordeste (UNNE), Resistencia, Argentina

2 Universidade Federal de Rio Grande do Sul (UFRGS), Laboratório de Aerodinâmica das Construções, Porto Alegre, Brazil

*Address all correspondence to: a_wittwer@yahoo.es

IntechOpen

© 2022 The Author(s). Licensee IntechOpen. This chapter is distributed under the terms of the Creative Commons Attribution License (<http://creativecommons.org/licenses/by/3.0>), which permits unrestricted use, distribution, and reproduction in any medium, provided the original work is properly cited. 

References

- [1] Arya S. In: Plate EJ, editor. *Atmospheric Boundary Layers over Homogeneous Terrain*. Engineering Meteorology. Amsterdam: Elsevier Scientific Publishing Company; 1982. pp. 233-266
- [2] Vento BJO. na Engenharia Estrutural. Editora da Universidade. Porto Alegre. Brazil: UFGRS; 1995
- [3] Kaimal JC, Wyngaard JC, Izumi Y, Cote OR. Spectral characteristics of surface-layer turbulence. *Quarterly Journal of the Royal Meteorological Society*. 1972;**98**:563-589
- [4] Kaimal JC. *Atmospheric Boundary Layer Flows: Their Structure and Measurement*. New York: Oxford University Press, Inc.; 1994
- [5] Cook NJ. Determination of the model scale factor in wind-tunnel simulations of the adiabatic atmospheric boundary layer. *Journal of Industrial Aerodynamics*. 1978;**2**:311-321
- [6] Hangan H. The WindEEE research institute and the WindEEE dome. In: *Wind EEE Scientific Symposium*. London, Canadá: Western University; 2013, 2013
- [7] Loredou-Souza AM, Rocha MM, Wittwer AR, Oliveira MK. Modelagem de edifícios altos em túnel de vento. *Concreto & Construções*. Revista do IBRACON - Instituto Brasileiro do Concreto. 2020;**99**:48-63
- [8] Blessmann J. The boundary layer TV-2 wind tunnel of the UFGRS. *Journal of Wind Engineering and Industrial Aerodynamics*. 1982;**10**:231-248
- [9] Wittwer AR, Möller SV. Characteristics of the low speed wind tunnel of the UNNE. *Journal of Wind Engineering & Industrial Aerodynamics*. 2000;**84**:307-320
- [10] Single Sensor Miniature Wire Probes. Dantec Dynamics. 2019. Available online: <https://www.dantecdynamics.com/productsand-services/single-sensor-miniature-wire-probes>. [Accessed: September 6, 2019]
- [11] Vosáhlo L. *Computer Programs for Evaluation of Turbulence Characteristics from Hot-Wire Measurements*. Karlsruhe: KfK 3743, Kernforschungszentrum Karlsruhe; 1984
- [12] Möller S. *Experimentelle Untersuchung der Vorgänge in engen Spalten zwischen den Unterkanälen von Stabbündeln bei turbulenter Strömung*. Dissertation. Karlsruhe. RFA. 1988; KfK 4501: Universität Karlsruhe (TH); 1989
- [13] Press WH, Flannery BP, Teukolsky SA, Vetterling WT. *Numerical Recipes: The Art of Scientific Computing*. New York: Cambridge University Press; 1990
- [14] Jensen M. The model law phenomena in natural wind. *Ingeniøren*. 1958;**2**: 121-128
- [15] Cermak JE. Laboratory simulation of the atmospheric boundary layer. *AIAA Journal*. 1971;**9**(9):1746-1754
- [16] Ruscheweyh H, Fisher K. Aerodynamic effects of large natural-draught cooling towers on the atmospheric dispersion from a stack. *Journal of Industrial Aerodynamics*. 1979;**4**:399-413
- [17] Counihan J. An improved method of simulating an atmospheric boundary layer in a wind tunnel. *Atmospheric Environment*. 1969;**3**:197-214

- [18] Standen NM. A Spire Array for Generating Thick Turbulent Shear Layers for Natural Wind Simulation in Wind Tunnels. National Research Council of Canada, National Aeronautical Establishment (NAE), Laboratory Technical Report LTR-LA-94. 1972
- [19] Isymov N, Tanaka H. Wind tunnel modelling of stack gas dispersion – Difficulties and approximations. Wind engineering. In: Cermak JE, editor. Proceedings of the Fifth International Conference. Fort Collins, Colorado, USA: Pergamon Press Ltd; 1979
- [20] Meroney R, Neff D. Laboratory simulation of liquid natural gas vapour dispersion over land or water. Wind engineering. In: Cermak J, editor. Proceedings of the Fifth International Conference. Vol. 2. Fort Collins, Colorado, USA: Pergamon Press Ltd; 1980. pp. 1139-1149
- [21] Janssen LAM. Wind tunnel modelling of dispersion of Odours in the neighborhood of pig houses. Journal of Industrial Aerodynamics. 1979;4:391-398
- [22] Wittwer A, Welter G, Loredou-Souza A. Statistical analysis of wind tunnel and atmospheric boundary layer turbulent flows. In: Wind Tunnel Designs and their Diverse Engineering Applications, book edited by N. A. Ahmed, ISBN 978-953-51-1047-7, . London, UK: INTECH; 2013
- [23] Wittwer A, Loredou-Souza A, De Bortoli M, Marighetti J. Physical models of atmospheric boundary layer flows: Some developments and recent applications. Book chapter in: Boundary Layer Flows - Theory, Applications and Numerical Methods (ISBN 978-1-83968-186-8). Book edited by: Vallamapati Ramachandra Prasad. London, UK: INTECH OPEN; 2019
- [24] Chamorro LP, Porté-Agel F. Effects of thermal stability and incoming boundary-layer flow characteristics on wind-turbine wakes: A wind-tunnel study. Boundary-Layer Meteorology. 2010;136:515-533
- [25] Demarco G, Puhales F, Acevedo OC, Costa FD, Avelar AC, Fisch G. Dependence of turbulence-related quantities on the mechanical forcing for wind tunnel stratified flow. American Journal of Environment Engineering. 2015;5:15-26
- [26] Puhales FS, Demarco G, Martins LGN, Acevedo OC, Degrazia GA, Welter GS, et al. Estimates of turbulent kinetic energy dissipation rate for a stratified flow in a wind tunnel. Physica A: Statistical Mechanics and its Applications. 2015;431:175-187
- [27] Arya SPS. Buoyancy effects in a horizontal flat-plate boundary layer. Journal of Fluid Mechanics. 1975;68:321-343
- [28] Williams O, Hohman T, Van Buren T, Bou-Zeid E, Smits AJ. The effect of stable thermal stratification on turbulent boundary layer statistics. Journal of Fluid Mechanics. 2017;812:1039-1075
- [29] Doosttalab A, Araya G, Newman J, Adrian RJ, Jansen K, Castillo L. Effect of small roughness elements on thermal statistics of a turbulent boundary layer at moderate Reynolds number. Journal of Fluid Mechanics. 2016;787:84-115
- [30] Kabir IFSA, Ng E. Effect of different atmospheric boundary layers on the wake characteristics of NREL phase VI wind turbine. Renewable Energy. 2019;130:1185-1197

[31] Demarco G, Martins LGN, Bodmann BEJ, Puhales FS, Acevedo OC, Wittwer AR, et al. Analysis of thermal and roughness effects on the turbulent characteristics of experimentally simulated boundary layers in a wind tunnel. *International Journal of Environmental Research and Public Health*. 2022;**19**:5134

IntechOpen

IntechOpen